Femtosecond Transient Hole-Burning Detection of Interexciton-State Radiationless Decay in Allophycocyanin Trimers

Maurice D. Edington, Ruth E. Riter,† and Warren F. Beck*

Department of Chemistry, Vanderbilt University, 5134 Stevenson Center, P.O. Box 1822-B, Nashville, Tennessee 37235

Received: February 4, 1997; In Final Form: April 8, 1997[⊗]

In its trimeric aggregation state, the phycobiliprotein allophycocyanin contains the simplest possible system, an isolated pair of chromophores, in which delocalized excited states can be studied. By moving the pump wavelength across allophycocyanin's ground-state absorption band, we have obtained femtosecond time-resolved pump−probe spectra that evidence interexciton-state radiationless decay from the upper exciton state and vibrational relaxation in the lower exciton state. Direct evidence for interexciton-state radiationless decay is taken from the initial appearance of photobleaching/stimulated-emission holes displaced to the red with respect to the pump-pulse spectrum. The holes broaden on the 120-fs time scale owing to intramolecular vibrational redistribution and transient solvation and shift to the red on the 230-fs time scale owing to vibrational equilibration and transient solvation. We show that vibrational relaxation in the lower exciton state contributes to the decay of a shoulder in the 590−640-nm region on the 400-fs time scale when 620-nm excitation is employed but not when the pump spectrum is tuned farther to the red, away from the $0 \rightarrow 1$ vibronic transition to the lower exciton state. In the absence of vibrational relaxation in the lower exciton state, we can now discern that exciton localization contributes to the time evolution in the 590−640-nm region of the spectrum on the 1-ps time scale.

Introduction

The pairing or clustering of chromophores in photosynthetic light-harvesting proteins[1−7] raises the possibility that delocalized electronic states play an important role in the dynamics of energy transfer.[8−10] Our work in this area has been initially concentrated on the dynamics exhibited by the phycobiliproteins allophycocyanin and *C*-phycocyanin. The structures of these proteins[2−4,6] can be described as ringlike homotrimers of α,β polypeptide monomers, each of which binds one phycocyanobilin chromophore. The chromophores are arranged as pairs on adjacent α,β monomers, resulting in a C_3 symmetric array of well-separated $\alpha 84-\beta 84$ chromophore dimers. The structure of *C*-phycocyanin differs slightly from allophycocyanin in that it contains one extra chromophore bound on the β subunit. These proteins have proven to be well-suited for fundamental energy-transfer studies on the chromophore dimers,[11,12] as well as for investigations of the excited-state photophysics of single phycocyanobilin chromophores in the isolated limit.[13]

We recently showed that the initially prepared excited state in allophycocyanin is delocalized over a given $\alpha 84-\beta 84$ pair.[11,12] The initially delocalized excited state is reported by the large initial anisotropy values[14−16] that we observed in a discrete two-color pump−probe anisotropy experiment[12] and by the appearance of the time-resolved pump−probe absorption-difference spectrum.[11] The time evolution of the pump−probe spectrum is dominated by interexciton-state radiationless decay. With excitation at 620 nm, a 650−660-nm photobleaching/stimulated emission (PB/SE) band promptly forms well red-shifted from the position of the pump-pulse spectrum. Discrete two-color pump−probe transients showed that the PB/SE band forms on the 35-fs time scale; a similar time scale was obtained from the fast phase of the anisotropy decay, which directly reports the time scale for interexciton-state relaxation.[17] The time scale for the relaxation from the upper exciton state to the lower exciton state is easily an order of magnitude shorter than the time scale predicted for Förster energy transfer[18] between the $\alpha 84$ and $\beta 84$ chromophores.[19−21]

A second phase of spectral evolution in the absorption-difference spectrum of allophycocyanin occurs on the 300−1000-fs time scale; a shoulder on the main PB/SE band, in the 590−640-nm region, decays away at the same time that the main 650−660-nm PB/SE band increases in intensity.[11] With the aid of calculated spectra, we showed that this slower phase of spectral evolution might involve localization of an exciton onto a single chromophore. We pointed out, however, that vibrational relaxation in the lower exciton state's vibronic manifold could also make a contribution to the spectral metamorphosis in the 590−640-nm region. The behavior observed in the time-resolved pump−probe spectrum exhibited by allophycocyanin trimers is strikingly similar to that calculated by Struve for chlorophyll *a* in solution following excitation of a $0 \rightarrow 1$ vibronic transition.[22]

The possibility that vibrational relaxation was involved was also prompted by our analysis of the ground-state absorption spectrum exhibited by allophycocyanin trimers. Figure 1 shows the absorption line shapes assigned to the upper and lower exciton-state transitions in our previous work.[11] Each band is modeled as the sum of log-normal line shapes[23] for the $0 \rightarrow 0$ and $0 \rightarrow 1$ vibronic transitions. The vibronic transition is positioned $\sim$1500 cm^{-1} to higher energy from the $0 \rightarrow 0$ transition, the spacing suggested by the strongest line in the Raman spectra reported by Lutz and co-workers[24,25] and by the spacing of the main and vibronic bands observed in the fluorescence-emission spectrum.[11,26] The vibronic structure is not as apparent in the band arising from the transition to the upper exciton state because of lifetime broadening. The pump pulses used in the previous work were centered at 620 nm, so

† Present address: Department of Chemistry, Colorado State University, Fort Collins, CO 80523.

⊗ Abstract published in *Advance ACS Abstracts,* May 15, 1997.

S1089-5647(97)00424-0 CCC: $14.00

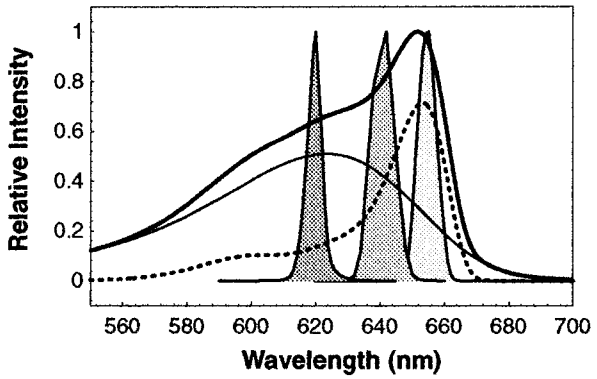

Figure 1. Continuous ground-state absorption spectrum (thick black curve) exhibited by allophycocyanin trimers at 22 °C with 2-nm spectral band-pass. The thin solid black and dashed black curves represent components assigned to the upper ($|+\rangle$)and lower ($|-\rangle$) exciton states, respectively. The intensity spectrum of the pump pulses used to obtain time-resolved spectra in Figures 2−4, centered at 620, 640, and 655 nm, respectively, are shown superimposed (gray filled curves, from left to right) for comparison.

the 0 → 1 vibronic transition to the lower exciton state was directly pumped.

By moving the pump wavelength across the ground-state absorption band, we have now obtained a series of time-resolved pump−probe spectra that evidence vibrational relaxation in the lower exciton state and interexciton-state radiationless decay from the upper exciton state. Direct evidence for the presence of interexciton-state relaxation processes in allophycocyanin is obtained in terms of *hole-burned* PB/SE line shapes that are displaced to the red with respect to the spectrum of the pump pulses. Vibrational relaxation clearly contributes to the time evolution of the time-resolved spectrum on the 400-fs time scale when the 0 → 1 vibronic transition to the lower exciton state is directly pumped. Interestingly, the spectra exhibit a slower time evolution on the 1-ps time scale that is consistent with exciton localization that we can now discern in the absence of vibrational relaxation. Thus, this paper provides further evidence that initially delocalized electronic states can decay to localized states on a time scale that is relevant to light-harvesting processes in the antenna/reaction center complex.

Experimental Section

Sample Preparation. Allophycocyanin trimers were isolated from cultures of the AN112 mutant of *Synechococcus* PCC 6301, as described elsewhere.[27] Allophycocyanin trimer preparations were concentrated over a PM-30 membrane in an Amicon ultrafiltration cell to obtain an absorbance of 0.3−0.4 when measured in a cell with a 1-mm path. The samples were stored in the dark at 4 °C suspended in a 100 mM sodium phosphate buffer solution at pH 7.0.

Femtosecond Spectroscopy. The femtosecond laser spectrometer we used to obtain time-resolved pump−probe absorption-difference spectra consists of an amplified colliding-pulse, mode-locked (CPM) dye laser, a modified Michelson pump−probe interferometer, and continuum-probe detection system that has been described in detail previously.[13] For experiments using 620-nm pump pulses, the output of the amplified CPM laser was used directly. For experiments using 640- and 655-nm excitation, the pump spectrum was selected from a femtosecond continuum with a three-cavity Fabry-Perot interference filter (Omega Optics). In all of the experiments, the pump beam was compensated for group-delay dispersion prior to arrival at the sample position with a pair of SF10 prisms. The probe beam was compensated for group-delay dispersion across the continuum's spectrum by scanning a computer-controlled translation stage in the pump beam's path so that the arrival delay for a given wavelength was nulled; the program for the translation stage was obtained from a study of the chirp on the continuum performed with a frequency-resolved cross-correlation or nonresonant optical Kerr technique, as described previously.[13] The continuum had sufficient intensity that time-resolved spectra could be measured over a range of 450−800 nm.

Discrete two-color pump−probe experiments were conducted as described previously.[12] The 655-nm pump beam was sliced from the continuum using an interference filter, as described above, and the probe beam was obtained directly from the amplified CPM laser.

In all of the experiments, neutral-density filters were used to attenuate the pump pulses to the 8−12 nJ/pulse level (at 3 kHz), as measured at the sample's position; owing to improved performance of the detection system and better laser stability, we were able to achieve a 4-fold reduction in the pump-pulse intensity compared to our previously reported work[11,12] while still improving the signal/noise ratio. In the time-resolved spectra, the probe pulses were attenuated to 4−5 nJ/pulse for the entire continuum. The two-color pump−probe experiment employed probe pulses set to 0.9 nJ/pulse. The pump−probe cross-correlation wave form exhibited 170-fs widths across the continuum in all of the time-resolved spectra and in the discrete two-color pump−probe experiments. The time-resolved spectra were acquired in 2-nm wavelength steps; the spectra were binned to reduce the resolution to 4 nm/point, in accord with the spectral band-pass of the grating spectrometer used to disperse the transmitted probe beam, but no other smoothing was applied. The spectra obtained with 655-nm pump pulses exhibited a scattered-light artifact, so we did not plot the spectra in the affected wavelength range.

Results

Figures 2−4 report time-resolved pump−probe absorption-difference spectra obtained with allophycocyanin trimers with the pump-pulse spectrum set to 620, 640, and 655 nm, respectively. As shown in Figure 1, this scan of the pump-pulse spectrum across the ground-state absorption spectrum of allophycocyanin would be expected to vary the ratio of populations initially prepared in the upper and lower exciton states from 4:1 to 1:3, with a 1:1 ratio achieved with 640-nm pump pulses. The scan also varies the vibronic state preparation in the lower exciton state. Whereas the 620-nm pump spectrum would be expect to stimulate both the 0 → 0 and the 0 → 1 vibronic transitions, pumping at 640 and 655 nm would be expected to hit only the 0 → 0 transition in the lower exciton state's vibronic manifold on the blue and red edges, respectively. Note that the 655-nm pump spectrum is located less than 100 cm^{-1} to higher energy with respect to the crossing of the continuous absorption and fluorescence-emission spectra.

The time-resolved spectra shown in Figures 2−4 share several common features. The most intense feature, a PB/SE band centered at long delays at 657 nm, grows in almost instantaneously. A region of net excited-state absorption (ESA) is observed in the 660−700-nm region. The following summary of the time evolution of the PB/SE band is based on the spectra shown in Figures 2−4 and others not shown at intermediate delays. The PB/SE band in the 650−660-nm region makes its appearance well red-shifted with respect to the pump spectrum in all three cases, even when 655-nm pump pulses are used. The final position of the PB/SE band is even more red-shifted; the band moves about 250 cm^{-1} to the red following an exponential with a 230-fs time constant when 620- and 640-

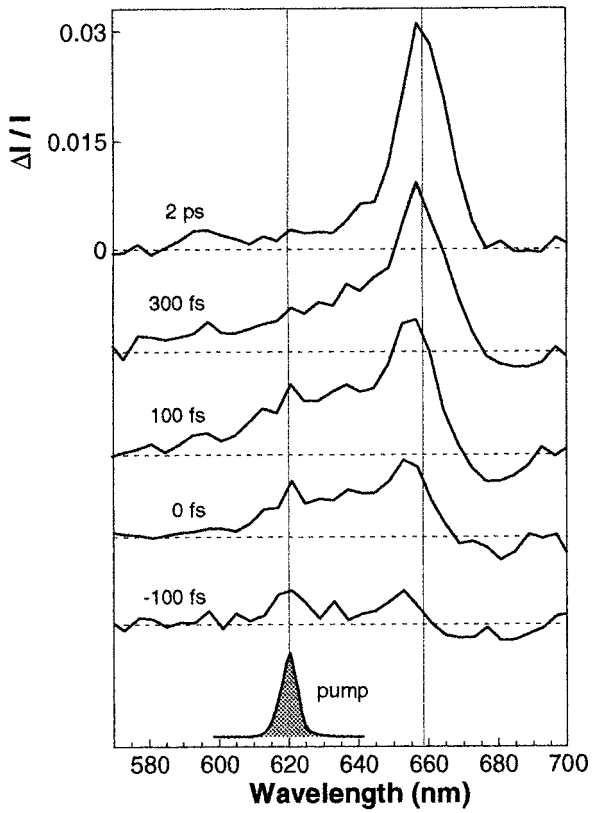

Figure 2. Time-resolved pump−probe absorption-difference spectra obtained in allophycocyanin trimers with 620-nm pump pulses at several probe delay times. The pump-pulse spectrum is shown below the spectra (shaded gray curve). The ordinate applies to the 2-ps spectrum; spectra obtained at other delays are vertically displaced arbitrarily but are displayed with the same scaling factor. The dashed horizontal lines mark the base line for each spectrum. The vertical lines mark the center of the pump-pulse spectrum and center of the PB/SE band in the 2-ps spectrum.

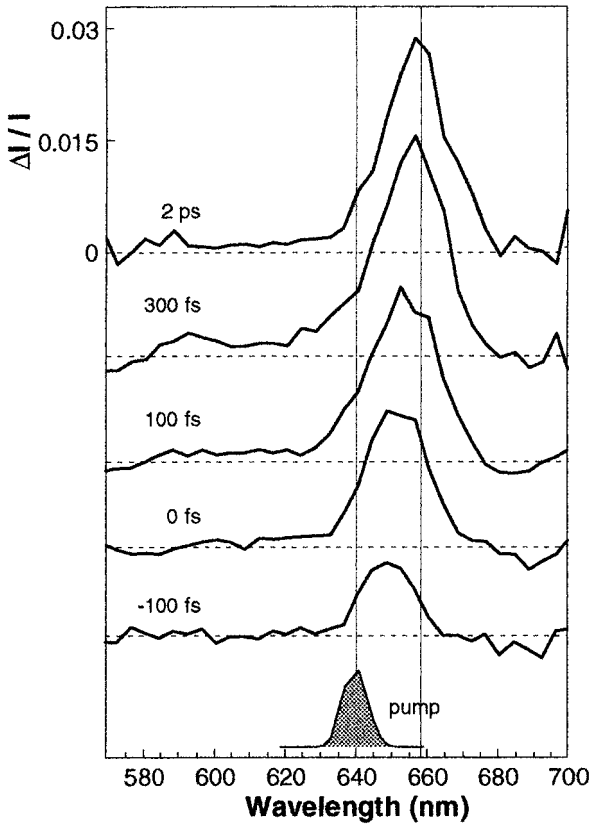

Figure 3. Time-resolved pump−probe absorption-difference spectra obtained in allophycocyanin trimers with 640-nm pump pulses at several probe delay times. The pump-pulse spectrum is shown below the spectra (shaded gray curve). The vertical lines mark the center of the pump-pulse spectrum and center of the PB/SE band in the 2-ps spectrum. Other details can be found in the legend to Figure 2.

nm pump pulses are used, and the band moves about 100 cm^{-1} to the red with the same time constant when 655-nm pump pulses are used. The ∼390-cm^{-1} initial width of the PB/SE band, as estimated with Gaussian line shapes, is significantly narrower at half-maximum than the final width of ∼510-cm^{-1}. The PB/SE band width broadens exponentially with time according to a ∼120-fs time constant.

The time-resolved spectra obtained with 620-nm pump pulses (Figure 2), however, are somewhat distinct from those observed with 640- or 655-nm pump pulses because a broad shoulder develops over the 590−640-nm region. The initial appearance of the 100-fs spectrum is that of a net PB/SE feature in the region of the 620-nm pump spectrum and a slightly more intense feature in the 652-nm region. Some of the intensity in the 620-nm region in the spectra spanning the −100 to +100-fs delay region originates from a pump−probe coherence signal rather than from population.[28] The 590−640-nm shoulder reaches its maximum intensity near the 100-fs delay point and decays in intensity with increasing delay; at the same time, the PB/SE band in the 650−660-nm region increases in intensity. This behavior was extensively discussed in the previous work; when probe light at 620 nm is used in a one-color pump−probe experiment, an exponentially decaying transient with a ∼400-fs time constant is observed.[11] The spectrum measured with a 300-fs probe delay differs from that obtained with 640-nm pump pulses at the same delay (Figure 3) only because of what is left of the decaying shoulder. No time evolution on this time scale is obtained when 640- or 655-nm pump pulses are employed.

All three sets of spectra, however, exhibit a time evolution on the ∼1-ps time scale. This time evolution is more apparent when two-color transients are obtained with probe light in the 590−640- and 650−670-nm regions. Figure 5 shows a pair of two-color pump−probe transients obtained with 655-nm pump pulses. The probe wavelengths, at 620 and 665 nm, monitor the decay of the weak net PB signal observed in the 590−640-nm region and the rise of the 650−660-nm PB/SE band, respectively. The decay in the 620-nm region is well described by a single exponential with a 1.2-ps time constant (Figure 5a), with about 10% of the intensity described by a nondecaying offset. The rising signal detected at 665 nm (Figure 5b) can be described using two rising exponentials with time constants of 63 fs (40%) and 1.2 ps (10%). These results show that a decay on the 1-ps time scale in the 590−640-nm region is accompanied by a small increase in intensity in the PB/SE band on the same time scale.

Discussion

The time-resolved pump−probe absorption spectra obtained with allophycocyanin trimers (Figures 2−4) starkly contrast with the spectra obtained with the α subunit of *C*-phycocyanin,[29] which contains a single phycocyanobilin chromophore.[6] The spectra obtained with the α subunit exhibit initially narrow PB/SE holes centered on the pump−pulse spectrum; subsequently, the holes broaden in the <200-fs time scale owing to spectral diffusion arising from intramolecular vibrational redistribution (IVR) and transient solvation dynamics,[30] and the SE contribution shifts to the red on the <100-fs time scale owing to transient solvation. The spectra obtained with allophycocyanin trimers initially exhibit *hole-burned* PB/SE line shapes well red-shifted with respect to the pump-pulse spectrum. This result provides

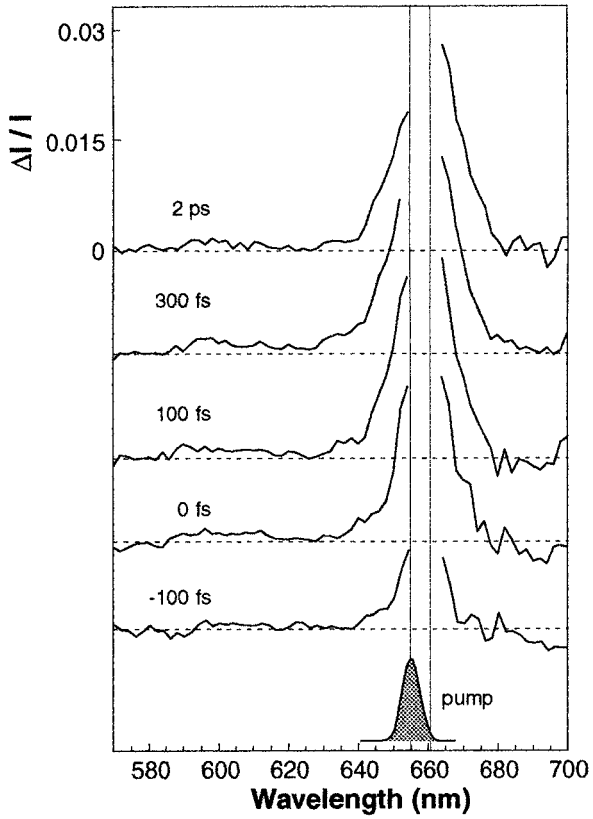

Figure 4. Time-resolved pump−probe absorption-difference spectra obtained in allophycocyanin trimers with 655-nm pump pulses at several probe delay times. The pump-pulse spectrum is shown below the spectra (shaded gray curve). The vertical lines mark the center of the pump-pulse spectrum and center of the PB/SE band in the 2-ps spectrum. The gap in the time-resolved spectra near 655 nm is present owing to a scattered-light artifact. Other details can be found in the legend to Figure 2.

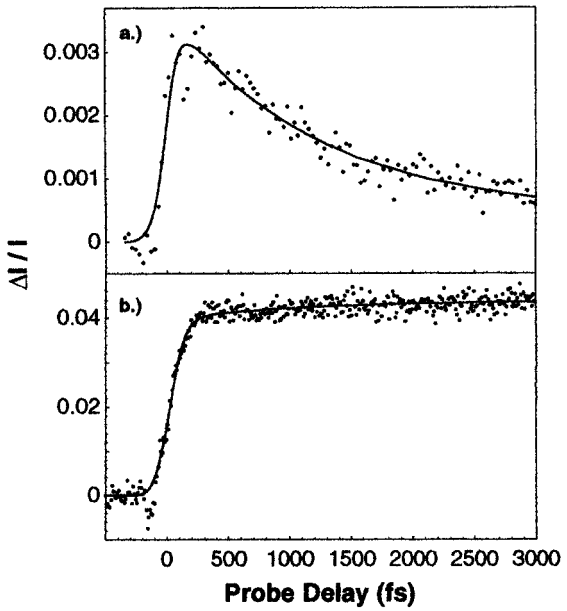

Figure 5. Pump−probe transients obtained with allophycocyanin trimers at ambient temperature (22 °C). Both transients are shown superimposed with a fit function obtained with an iterative reconvolution program. Top panel: Discrete two-color transient obtained with 655-nm pump and 620-nm probe pulses. The model used to describe the transient was $a_\infty + a_1 \exp(-t/\tau_1)$, where $a_1 = 0.89$, $\tau_1 = 1.2$ ps, and $a_\infty = 0.11$. Bottom panel: Two-color transient obtained with 620-nm pump and continuum-probe pulses, with detection at 665 nm. The model used to describe the transient was $a_\infty + \sum_{i=1}^{2} a_i \exp(-t/\tau_1)$, where $a_1 = -0.40$, $\tau_1 = 63$ fs, $a_2 = -0.10$, $\tau_2 = 1.2$ ps, and $a_\infty = 1.00$ (where the amplitudes of the rise components ($a_i < 0$) have been normalized to α_∞). The value for τ_2 was held fixed during the fit.

direct evidence for interexciton-state radiationless decay on a shorter time scale than that of spectral diffusion. In fact, owing to the much improved signal/noise ratio achieved in the current spectra compared to that of our previously reported spectra, we now observe line broadening and a dynamic Stokes shift arising from vibrational equilibration and transient solvation on a time scale that is comparable to that observed for those processes in the α-subunit system.

The inhomogeneously broadened character of the absorption transitions to the two exciton states exhibited by allophycocyanin trimers causes the initial appearance of the time-resolved spectra to be sensitive to the pump-pulse spectrum. As indicated in Figure 1, we suggest that the two absorption transitions overlap over nearly the entire width of the ground-state absorption spectrum, so the initial excited-state population will be partitioned between the two exciton states. The two exciton-state populations are initially confined to the same energy region because they are selected from the ground-state population by a relatively narrow pump-pulse spectrum. Population initially deposited in the lower exciton state can relax further only by vibrational equilibration and transient solvation. Owing to correlation of the energies of the exciton states *for a given chromophore dimer*, population initially deposited in the upper exciton state can relax to lower energy by radiationless decay to the corresponding lower exciton state. Correlation of exciton-state energies was previously detected in low-temperature persistent hole-burning experiments by Small and co-workers on the exciton states of the special-pair Q_y state of the reaction centers of *Rhodopseudomonas viridis* and *Rhodobacter sphaeroides*;[31] a similar state correlation and interexciton-state decay was detected in the bacteriochlorophyll *a* protein of *Prothecochloris aestuarii* by Small and co-workers.[32]

This model suggests that *two* PB/SE holes might initially be observed in the time-resolved pump−probe spectrum *if* the pump wavelength is tuned far enough away from the bottom of the lower exciton state's vibronic manifold. It is possible that we observe two holes transiently in the set of spectra obtained with 620-nm excitation (Figure 2), but a contribution from four-wave mixing unrelated to population cannot be easily excluded. The hole near the pump-pulse spectrum would arise from the population initially placed in the lower exciton state; the hole displaced to lower energy would arise following interexciton-state radiationless decay from the population initially placed in the upper exciton state. As the pump-pulse spectrum is tuned to lower energy, the model predicts that the two holes should merge, as is apparently observed when 640- and 655-nm pump pulses are employed (Figures 3 and 4). Owing to state correlation, the red side of the merged hole should always be to the red of the pump spectrum; the blue side of the merged hole should track the pump-pulse spectrum. Both expectations are met in the time-resolved spectra shown in Figures 2−4.

When the pump-pulse spectrum is centered at 620 nm, but not at 640 or 655 nm, the time-resolved pump−probe spectra obtained with allophycocyanin trimers exhibit a time evolution on the 400-fs time scale (see Figure 2) that evidently involves vibrational relaxation of population initially placed in the lower exciton state. When 620-nm pump pulses are used, the time-resolved spectra exhibit a shoulder over the 590−640-nm region that persists over the 0−300-fs delay region. The decay of the shoulder is accompanied by a rise in the large PB/SE band in the 655-nm region on the 400-fs time scale; single-wavelength transients showing these spectral dynamics are documented in

our previously published work.[11] Figures 3 and 4 show that the 590−640-nm shoulder is not observed when excitation is moved to the 640- or 655-nm position. The pump-wavelength sensitivity of the shoulder confirms the presence of a $0 \rightarrow 1$ vibronic transition to the lower exciton state. The presence of the vibronic transition was deduced previously by considering the asymmetry of the continuous fluorescence-emission spectrum. Owing to the extraordinarily rapid interexciton-state radiationless decay, only the lower exciton state emits fluorescence. By applying mirror symmetry and a Stokes shift judged from continuous spectra, we constructed the absorption line shape for the lower exciton state (as shown in Figure 1).[11] The behavior of the time-resolved spectra following excitation of the $0 \rightarrow 1$ vibronic transition is exactly as expected by theory. As discussed by Struve[22] with respect to chlorophyll *a*, excitation of a $0 \rightarrow 1$ vibronic transition will result in a visible decrease in the pumped region and an increase in the region of the $0 \rightarrow 0$ transition owing to vibrational relaxation if the Huang−Rhys factor for the mode is large enough. Judging again from the shape of the fluorescence-emission spectrum, the area of the $0 \rightarrow 1$ vibronic transition accounts for 20−30% of the oscillator strength.

Even when the $0 \rightarrow 1$ vibronic transition to the lower exciton state is not pumped directly, as in experiments involving 640- or 655-nm pump-pulse spectra, the time-resolved pump−probe spectra evolve on a slower time scale so that the 590−640-nm region decreases in intensity and the PB/SE band in the 655-nm region increases in intensity. This time evolution is most clearly visualized by the 1.2-ps exponential decay exhibited by the single-probe-wavelength transient shown in Figure 5, where 655-nm pump pulses and 620-nm probe pulses were employed. This sort of time evolution, as characterized by a collapse of the spectrum to lower energy even when the most red-shifted portion of the ground-state absorption spectrum is excited, is not easily explained by vibrational equilibration. Our previously reported calculations of allophycocyanin's time-resolved pump−probe spectra assigned this sort of time evolution to exciton localization. The SE and ESA contributions to the time-resolved pump−probe spectra evolve when the initially delocalized state collapses onto one of the chromophores in a given $\alpha 84-\beta 84$ dimer because the oscillator strength initially distributed into the transitions of the exciton states is redistributed to the site (isolated-chromophore) transitions.[11] The degree of mixing of the two site states was overestimated in the previous work because the calculations did not allow for the possibility of vibrational relaxation on the sub-picosecond time scale. The present results suggest that about half of the decay of the 590−640-nm shoulder feature in the time-resolved spectra involves vibrational relaxation when 620-nm pump pulses are used. This finding suggests that the estimate of 220 cm^{-1} for the dipole−dipole interaction energy for the $\alpha 84-\beta 84$ dimer estimated from the behavior of the calculated spectra should be decreased to $\sim$150 cm^{-1} so that the shift in oscillator strength from exciton to localized states is decreased. This value for the dipole−dipole interaction energy is more in line with that estimated from circular dichroism spectra.[33]

In summary, the present work supports the previous conclusion that the excited electronic states in allophycocyanin trimers are delocalized in character by showing that hole-burned PB/SE features that are well red-shifted with respect to the pump-pulse spectrum are formed on a time scale that is short compared to that of spectral diffusion. For the first time, we are able to distinguish between dynamics associated with vibrational relaxation and slower dynamics that may involve localization. These findings add further weight to the idea that the dominant photophysics in coupled chromophore arrays in photosynthetic light-harvesting proteins involve interexciton-state radiationless decay.

Acknowledgment. This work was supported by grants from the Petroleum Research Fund (administered by the American Chemical Society), the Searle Scholars Program (the Chicago Community Trust), and the United States Department of Agriculture (NRIGCP). Additional support came from a Cottrell Scholars Award to W.F.B. (from the Research Corporation). M.D.E. was supported by a graduate fellowship from the David and Lucile Packard Foundation.

References and Notes

(1) Tronrud, D. E.; Schmid, M. F.; Matthews, B. W. *J. Mol. Biol.* **1986**, *188*, 443−454.

(2) Schirmer, T.; Bode, W.; Huber, R.; Sidler, W.; Zuber, H. *J. Mol. Biol.* **1985**, *184*, 257−277.

(3) Schirmer, T.; Huber, R.; Schneider, M.; Bode, W.; Miller, M.; Hackert, M. L. *J. Mol. Biol.* **1986**, *188*, 651−676.

(4) Schirmer, T.; Bode, W.; Huber, R. *J. Mol. Biol.* **1987**, *196*, 677−695.

(5) Kühlbrandt, W.; Wang, D. N. *Nature* **1991**, *350*, 130−134.

(6) Brejc, K.; Ficner, R.; Huber, R.; Steinbacher, S. *J. Mol. Biol.* **1995**, *249*, 424−440.

(7) McDermott, G.; Prince, S. M.; Freer, A. A.; Hawthornthwaite-Lawless, A. M.; Papiz, M. Z.; Cogdell, R. J.; Isaccs, N. W. *Nature* **1995**, *374*, 517−521.

(8) Sauer, K. In *Bioenergetics of Photosynthesis*; Govindjee, Ed.; Academic Press: New York, 1975; pp 115−181.

(9) van Grondelle, R. *Biochim. Biophys. Acta* **1985**, *811*, 147−195.

(10) van Grondelle, R.; Dekker, J. P.; Gillbro, T.; Sundström, V. *Biochim. Biophys. Acta* **1994**, *1187*, 1−65.

(11) Edington, M. D.; Riter, R. E.; Beck, W. F. *J. Phys. Chem.* **1996**, *100*, 14206−14217.

(12) Edington, M. D.; Riter, R. E.; Beck, W. F. *J. Phys. Chem.* **1995**, *99*, 15699−15704.

(13) Riter, R. E.; Edington, M. D.; Beck, W. F. *J. Phys. Chem.* **1996**, *100*, 14198−14205.

(14) Knox, R. S.; Gülen, D. *Photochem. Photobiol.* **1993**, *57*, 40−43.

(15) Wynne, K.; Hochstrasser, R. M. *Chem. Phys.* **1993**, *171*, 179−188.

(16) Matro, A.; Cina, J. A. *J. Phys. Chem.* **1995**, *99*, 2568−2582.

(17) van Amerongen, H.; Struve, W. S. *Methods Enzymol.* **1995**, *246*, 259−283.

(18) Förster, T. In *Modern Quantum Chemistry: III. Action of Light and Organic Crystals*; Sinanoglu, O., Ed.; Academic Press: New York, 1965; pp 93−137.

(19) Sauer, K.; Scheer, H.; Sauer, P. *Photochem. Photobiol.* **1987**, *46*, 427−440.

(20) Sauer, K.; Scheer, H. *Biochim. Biophys. Acta* **1988**, *936*, 157−170.

(21) Sauer, K.; Scheer, H. In *Photosynthetic Light-Harvesting Systems*; Scheer, H., Schneider, S., Eds.; Walter de Gruyter: Berlin, 1988; pp 507−511.

(22) Struve, W. S. *Biophys. J.* **1995**, *69*, 2739−2744.

(23) Siano, D. B.; Metzler, D. E. *J. Chem. Phys.* **1969**, *51*, 1856−1861.

(24) Szalontai, B.; Gombos, Z.; Csizmadia, V.; Csatorday, K.; Lutz, M. *Biochemistry* **1989**, *28*, 6467−6472.

(25) Szalontai, B.; Gombos, Z.; Csizamadia, V.; Bagyinka, C.; Lutz, M. *Biochemistry* **1994**, *33*, 11823−11832.

(26) Xie, X.; Du, M.; Mets, L.; Fleming, G. In *Time-Resolved Laser Spectroscopy in Biochemistry III*; SPIE: Bellingham, 1992; pp 690−706.

(27) Glazer, A. N.; Fang, S. *J. Biol. Chem.* **1973**, *248*, 659−662.

(28) Kang, T. J.; Yu, J.; Berg, M. *J. Chem. Phys.* **1991**, *94*, 2413−2424.

(29) Riter, R. E.; Edington, M. D.; Beck, W. F. In *Ultrafast Phenomena X*; Barbara, P., Knox, W., Zinth, W., Fujimoto, J., Eds.; Springer-Verlag: Berlin, 1996; pp 324−326.

(30) Loring, R. F.; Yan, Y. J.; Mukamel, S. *J. Chem. Phys.* **1987**, *87*, 5840−5857.

(31) Johnson, S. G.; Tang, D.; Jankowiak, R.; Hayes, J. M.; Small, G. H. *J. Phys. Chem.* **1989**, *93*, 5953−5957.

(32) Johnson, S. G.; Small, G. J. *J. Phys. Chem.* **1991**, *95*, 471−479.

(33) Csatorday, K.; MacColl, R.; Csizmadia, V.; Grabowski, J.; Bagyinka, C. *Biochemistry* **1984**, *23*, 6466−6470.